Molecular Mechanisms of Danhong Injection in Treatment of Pulmonary Fibrosis Based on Network Pharmacology and Experimental Validation

Di Han
Affiliated Hospital of Nanjing University of Chinese Medicine: Jiangsu Province Academy of Traditional Chinese Medicine

Yong Xu
Affiliated Hospital of Nanjing University of Chinese Medicine: Jiangsu Province Academy of Traditional Chinese Medicine

Wenpan Peng
Affiliated Hospital of Nanjing University of Chinese Medicine: Jiangsu Province Academy of Traditional Chinese Medicine

Dan Wang
Affiliated Hospital of Nanjing University of Chinese Medicine: Jiangsu Province Academy of Traditional Chinese Medicine

Tongxing Huang
Affiliated Hospital of Nanjing University of Chinese Medicine: Jiangsu Province Academy of Traditional Chinese Medicine

Xianmei Zhou
Affiliated Hospital of Nanjing University of Chinese Medicine: Jiangsu Province Academy of Traditional Chinese Medicine

Jinjun Shan (jshan@njucm.edu.cn)
Jiangsu key laboratory of pediatric respiratory disease; Institute of Pediatrics https://orcid.org/0000-0001-8079-7950

Research

Keywords: Danhong injection, Pulmonary fibrosis, network pharmacology, Pi3k/Akt, apoptosis

Posted Date: June 11th, 2021

DOI: https://doi.org/10.21203/rs.3.rs-590776/v1

Molecular mechanisms of Danhong injection in treatment of Pulmonary Fibrosis based on network pharmacology and experimental validation

Di Han[1,2†], Yong Xu[1,2†], Wenpan Peng[1,2], Dan Wang[1,2], Tongxing Huang[1,2], Xianmei Zhou[1,2*] and Jinjun Shan[3,4*]

[*]Correspondence: zhouxianmeijs@aliyun.com；jshan@njucm.edu.cn
[†]Di Han and Yong Xu contributed equally to this work
[1] Affiliated Hospital of Nanjing University of Chinese Medicine, Nanjing, 210023 China
Full list of author information is available at the end of the article

Abstract

Backgroud: Danhong injection has been proven to be reliable and practical in the clinical treatment of Pulmonary Fibrosis (PF), whereas the mechanism of action is unclear. The aim of this study was to investigate the mechanism of action of Danhong injection in the treatment of PF through network pharmacology and experimental validation.

Methods: In this paper, multiple databases were utilized to capture the targets of Danhong injection and PF disease-related targets. The interaction network such as active ingredient-target was constructed and protein interaction analysis was performed via Cytoscape software. Bioprocess and signaling pathway analysis of the targets was carried out through DIVID database. Based on the analytical results, pharmacodynamic validation and mechanistic investigation were conducted in mice.

Results: In this study, 111 compounds and common targets for diseases were filtered, with key targets involving MDM2, IL-2, CCL5, AKT1, MMP9, CASP3, MMP2, etc.

The KEGG and GO enrichment analysis identified 16 significantly different signaling pathways, encompassing bioprocesses such as cell proliferation, apoptosis, programmed death and immune response. Animal experiments demonstrated that Danhong injection could reduce bleomycin-induced PF in mice, and could decrease the mRNA of AKT1 and the protein expression of p-Pi3k and p-Akt, thereby reducing apoptosis in mouse lung tissues.

Conclusions: This study initially revealed that Danhong injection may inhibit apoptosis through the Pi3k/Akt signaling pathway and thus reduce PF in mice.

Keywords: Danhong injection; Pulmonary fibrosis; network pharmacology; Pi3k/Akt; apoptosis

Backgroud

Among chronic respiratory diseases, Pulmonary Fibrosis (PF) is another "killer" in addition to lung cancer, which severely affects the quality of life among patients and significantly increases the economic burden on families and society[1]. Previous studies have demonstrated that the survival period for patients diagnosed with PF is only 2-3 years, with a 5-year survival rate of less than 30%[2]. Although PF is a rare disease, the morbidity and mortality rates are increasing every year with no effective drugs available[3].

PF is classified as ‘consumptive lung disease’ and ‘Bi syndrome of Lung’ in Chinese medicine, with ‘Bi syndrone of Lung’ predominating in the early stage and ‘consumptive lung disease’ developing in the late stage[4]. The disease pathogenesis is

essential empty and out solid. The essential empty is a deficiency of the lung, spleen and kidney, while the out solid is a paralysis of the lung channels by phlegm, heat and stasis. It is recognizedthat stagnated blood is a constant factor throughout the development of PF, thus PF can be treated based on the stagnated blood[5]. Traditional Chinese medicine features multi-component, multi-target and multi-pathway, and is widely used for its unique advantages in the treatment of sophisticated diseases[6]. Danhong injection is composed of Radix Salviae and Carthami Flos. Radix Salviae is bitter and slightly cold in nature, while Carthami Flos is pungent and warm in nature. The two drugs complement each other and work together to activate blood circulation, remove blood stasis, open the veins and relax the ligaments. According to extensive clinical studies, Danhong injection can improve the overall clinical efficiency, improve lung function, and diminish inflammatory response[7].

In this study, a "herbal-active component-target-disease" network was constructed through network pharmacology and experimental validation to investigate the active components and potential targets of Danhong injection for the treatment of PF, and to validate them through animal experiments.

Materials and Methods

Databases

Traditional Chinese Medicine Systems Pharmacology Database and Analysis Platform (TCMSP, http://tcmspw.com/tcmsp.php), Traditional Chinese Medicines Integrated Database (TCMID, http://119.3.41.228:8000/tcmid/), Similarity ensemble approach (SEA, http://sea.bkslab.org), SwissTargetPrediction databases (http://ww

w.swisstargetprediction.ch), Universal Protein (UniProt, http://www.uniprot.org/), DAVID Bioinformatics Resources (https://david.ncifcrf.gov/), STRING databases (https://string-db.org), Online Mendelian Inheritance in Man (OMIM, http://www.omim.org/), GeneCards (http://www.genecards.org), Pharmmapper (http://www.lilab-ecust.cn/pharmmapper/), Comparative Toxicogenomics Database (CTD, http://www.genecards.org), Therapeutic Target Database (TTD, http://bidd.nus.edu.sg/group/ttd/ttd.asp).

Acquisition of potential targets

The TCMSP, TCMID, SEA and SwissTargetPrediction databases were accessed for the active ingredients and potential targets of Salvia and Safflower. The OMIM, GeneCards, CTD and TTD databases were accessed for disease-related targets, with the search term "Pulmonary Fibrosis". The VennDiagram package in R was applied to obtain common targets by mapping drug potential targets to disease-related targets.

Plotting network and PPI diagrams

In this study, the files "Drug_Disease.txt", "network.txt" and "type.txt" were imported into the Cytoscape software. Cytoscape software was used to draw the network diagrams, and the common target information was imported into String Online Analysis Platform with the minimum confidence set to 0.9 for protein-protein interaction analysis, and the generated "string_interactions.tsv" file into Cytoscape software for topological analysis. The core targets with values greater than their mean values were

selected based on degree and betweenness centrality.

Enrichment analysis

In order to describe and annotate the functions of the target genes and to explore the signaling pathways involved, the core targets screened in 1.4 were subjected to GO and KEGG enrichment analyses through the DAVID database for the selected species "Homo sapiens". The GO enrichment analysis consisted of Molecular Function (MF), Biological Process (BP) and Cellular Components (CC). The results of both GO and KEGG enrichment analyses were filtered with a corrected P value (FDR) <0.05.

Experimental validation

Reagents and antibodies

The primary antibodies used in this study included antibodies to p-Pi3k, Pi3k, p-Akt, Akt, and β-tubulin purchased from CST (Danvers, Massachusetts, U.S.). Danhong injection (Shandong Buchang Pharmaceutical) was purchased from Jiangsu Provincial Hospital of Traditional Chinese Medicine (Nanjing, China). Bleomycin sulphate was purchased from TCI (Tokyo, Japan).

Animal models

Fifty male C57/BL6 mice were randomly divided into a normal control group, a model group, a Danhong injection group and a positive drug group, with 10 mice in each group. The normal control group was left untreated, and the rest of the groups were treated

with a single intratracheal dose of bleomycin at a concentration of 5 mg/ml. On the following day after operation, the normal control and model control groups were given saline gavage, the positive drug group was given pirfenidone 300ml/kg/d by gavage, and the Danhong injection group was given Danhong injection 3ml/kg/d and 6ml/kg/d by intraperitoneal injection once a day for 21 d. The body weight of the mice was weighed every 3 days to observe the changes in body weight. Three hours after the last dose, the mice were killed by cervical dissection and the lung tissues were stored at -80 ℃.

Haematoxylin and eosin (H&E) staining and Masson staining

Lung tissues were fixed with 4% neutral-buffered formalin for 24 h. After that the colon was eluted with gradient ethanol and then immersed in xylene for 1 h. The paraffin-embedded lung samples were sliced into 4-μm-thick sections, stained with haematoxylin and eosin, imaged under a light microscope for routine histopathological examination.

After dewaxing, sectioned samples was stained with hematoxylin for 30 s, hydrochloric acid to induce differentiation into blue, Masson compound staining solution for 2 min, 1% phosphomolybdate and bright green staining solution for 5 min, respectively. The sections were washed 3 times with 0.2% acetic acid after each staining, then dehydrated with anhydrous alcohol, cleaned with xylene until transparent, and sealed tightly with neutral glue. Images were obtained at 20× the original magnification.

Immunohistochemistry (IHC)

For immunohistochemical analysis, paraffin-embedded lung tissue sections were de-paraffined and antigens removed. The following experimental steps were performed according to the instructions of the UltraSensitive™sp immunohistochemical staining kit (MAIXIN.BIO, Fuzhou, China). Sections were stained with DAB solution (MAIXIN.BIO) and then re-stained with hematoxylin. Collagen I and collagen III expression was quantified by Image J.

Lung function tests

After anesthesia, the mice were fixed supine on the operating table. The trachea was exposed and a cannula was inserted into the trachea and secured with cotton thread. After transferring the mice to a body description platform, lung compliance and lung resistance were measured.

RNA isolation and quantitative real-time PCR (qRT-PCR)

Total RNA was extracted using Trizol reagent (Invitrogen; Carlsbad, CA) in accordance with the manufacturer's instructions. cDNA was obtained via reverse transcription, which was performed using the 5× All-in-One RT MasterMix (Applied Biological Materials Inc; Richmond, Canada). mRNA expression levels were analyzed via quantitative real-time PCR using EvaGreen 2× qPCR Master Mix (Applied Biological Materials Inc; Richmond Canada). Relative mRNA expression levels of target genes were determined by normalizing values to expression levels of GAPDH. Data analysis

was conducted using the comparative ΔΔCT method. The following primers were synthesized by Sangon Biotech (Shanghai, China). The primer sequence is shown in Table 1.

Western Blotting (WB)

The lung tissue was lysed in RIPA containing 1% PMSF (Beyotime, Nanjing, China), and total protein levels were determined using the pierce BCA protein analysis kit (Thermo Scientific; Rockford, IL). Proteins (20 g/well) were separated via SDS-polyacrylamide gel electrophoresis and subsequently transferred to a PVDF membrane (Merck MILI; Darmstadt, Germany). Subsequently, the membrane was incubated with 5% skim milk in Tris-buffered saline containing 0.1% Tween 20 (TBST 25℃ for 1 h. Then, the membrane and primary antibody were incubated overnight at 4℃. Proteins were detected by incubating with a rabbit or mouse IgG (H + L) antibody labeled with a peroxidase enzyme (Plano, TX). Visualization of target bands was accomplished using a super ECL detection kit (Yeasen; Shanghai, China). Protein levels were standardized using β-tubulin

Enzyme-linked immunosorbent assay (ELISA)

Levels of Hydroxyproline、Caspase -3、Caspase-8、Caspase-9 within the mouse lung tissue were determined using ELISA kits (Nanjing Jiancheng Bioengineering Institute, China). Results are based on three experiments.

TUNEL assay

The detection procedure was performed according to the manufacturer's instructions, but with modifications. Deparaffinized 4-μm-thick tissue sections were treated with 20 μg/ml proteinase K for 15 min at room temperature. Subsequently, the TUNEL reagent containing dUTP and TdT (Roche Diagnostics) was added to each section, and incubated in a humidified chamber at 37°C for 60 min. The sections were rinsed with PBS and the sections were incubated with 0.3% converter-peroxidase for 30 min at 37°C, then the sections rinsed with PBS prior to the addition of DAB substrate 10 min at room temperature and color rendering was observed under the microscope for 3–8 min. After the color development with tap water, sections were rinsed for 15 min and hematoxylin staining was performed for 2 min at room temperature, and subsequent steps were performed as follows. At the room temperature, the sections rinsed with tap water and differentiated with hydrochloric acid alcohol for 3–8 sec, then the slices were immersed in 70% alcohol at 5 min, 80% alcohol at 5 min, 90% alcohol at 5 min and 100% alcohol at 5 min twice, soaked in xylene at 10 min twice, and sealed with neutral balsam. The sections were observed by light microscopy (magnification, 20×).

Data analysis

The ggplot2, ggpubr, Rmisc and ComplexHeatmap data packages in R language software were used for statistical analysis and visualization; one-way ANOVA was used for comparative analysis using Graphpad Prism software, expressed as mean ± standard deviation ($\bar{x}\pm s$). $p<0.05$ indicates a statistically significant difference.

Results

Active ingredients and potential targets of Danhong injection

Under the limited conditions of OB≥30% and DL≥0.18%[8], a total of 85 active ingredients were obtained by searching the TCMSP database for the two herbal medicines of Radix Salviae and Carthami Flos (Table 2), of which 65 were from Radix Salviae and 22 from Carthami Flos. luteolin and Baicalin were common to both Salvia miltiorrhiza and Safflower. The highest bioavailability was obtained from (2R)-3-(3,4-dihydroxyphenyl)-2-[(Z)-3-(3,4-dihydroxyphenyl)acryloyl]oxy-propionic acid of Radix Salviae. The compounds collected were de-weighted and finally screened for 84 active ingredients (Table.2). The OB is the proportion of the administered drug that enters the body's circulation and describes the percentage of the oral dose that is absorbed by the gastrointestinal tract and passes through the liver to reach the bloodstream in the body's circulation, while the DL refers to the similarity of the compounds to known drugs.

Drug-disease intersection targets

A total of 599 Salvia miltiorrhiza and safflower-related targets and 5311 PF-related targets were obtained through database screening. The potential targets of Salvia and Safflower were mapped to PF-related targets, and 111 common targets were obtained and made into a Venn diagram (Fig. 2).

Anti-PF network diagram of the active ingredients of Danhong injection

In the drug-target-disease network diagram, the blue nodes represent the active

ingredient information, the purple nodes represent the signaling pathways, the red nodes represent the drug and the green nodes represent the target information. A topological analysis of the network diagram revealed that there were 120 nodes and 1306 connecting lines, with a network centralization of 0.597, network heterogeneity of 1.006 and network density of 0.177(Fig.3).

Screening of the core targets of the active ingredient of Danhong injection against PF

The number of nodes connected represents the degree value and the median centrality represents the core degree of the node in the disease, both of which are important indicators to describe the nodes. The 111 common targets obtained in 2.2 were imported into the String online analysis platform, PPI maps were created and topological analysis was performed, and nodes with degree and median centrality greater than their mean values were retained as core targets. The results showed that a total of 21 core targets were filtered (Fig.4).

Anti-PF enrichment analysis of the active ingredients of Danhong injection

GO enrichment analysis (BP: 20, CC: 2, MF: 12) showed that the effects of Danhong injection were related to cell proliferation and apoptosis, cell bioregulation, cell biosynthesis, nucleic acid metabolic processes and protein transcription and translation (Fig. 5a); KEGG results showed that a total of 16 signaling pathways were closely related to PF, namely Pi3k/Akt signaling pathway, Chemokine signaling pathway, Thyroid hormone signaling pathway, Jak-STAT signaling pathway, GnRH signaling

pathway, ErbB signaling pathway, Rap1 signaling pathway, Ras signaling pathway, NF signaling pathway, FoxO signaling pathway, VEGF signaling pathway, Apoptosis, MAPK signaling pathway, HIF-1 signaling pathway, Toll-like receptor signaling pathway, T cell receptor signaling pathway (Fig. 5b).

Danhong injection attenuates bleomycin-induced PF in mice

The mouse model of bleomycin-induced PF has a large amount of inflammatory factors released, especially in the pre-fibrotic stage of lung formation[9]. After modelling, we selected the same tissues from the same areas for HE and Masson staining, and found that the alveolar structure of the mice was obviously destroyed, with a large number of inflammatory cells infiltrating and a large amount of blue collagen deposited in the alveolar septum and interstitial lung. Danhong injection was able to alleviate the inflammation and collagen deposition, and the effect was more obvious at higher doses (Fig. 6a). Danhong injection had no effect on the body weight of mice with PF (Fig. 6b). Testing of lung function in mice revealed that Danhong injection was able to improve lung function and increase lung compliance by reducing lung resistance (Fig. 6c, d).

Dan Hong Injection reduced collagen deposition in the lungs of mice with bleomycin-induced PF

Collagen content in lung tissue is a key indicator for evaluating PF[10]. Immunohistochemical results showed that collagen deposition was significant in the

model group compared to the normal control group and was improved in the high-dose group of mice after intervention with Danhong injection, with no significant difference in the low-dose group (Fig. 7a, b, c). Hydroxyproline is a non-essential amino acid found in collagen and some other extracellular animal proteins and plays a crucial role in the synthesis of collagen and in the thermodynamic stability of the triple helix conformation of collagen and associated tissues[11]. The detection of hydroxyproline content in mouse lung tissues revealed that the highest level of hydroxyproline was found in the lung tissues of mice in the model group, and that the level of hydroxyproline in the lung tissues of mice decreased after intervention with high doses of Danhong injection (Fig. 7d). The above results suggest that Danhong injection is sufficient to reduce collagen deposition in mice with PF to a certain extent.

Effect of Danhong injection on the transcription of key target genes in lung tissue of mice with PF

The above results have confirmed that Danhong injection can alleviate the inflammatory response and reduce collagen deposition to alleviate PF, but its mechanism is still unclear. Based on the results of the raw signal analysis, we predicted the mechanism of the anti-PF effect of Danhong injection. The expression of key target genes in the results was analyzed by extensive qRT-PCR assays. The results suggested that the genes with differences were MDM2, IL-2, CCL5, AKT1, MMP9, CASP3, MMP2 (Fig. 8).

Danhong injection exerts antifibrotic effects via Pi3k/Akt signaling pathway

We have screened the key targets of Danhong injection against PF by q-PCR, and combined with the results of KEGG enriched signaling pathway, we found that Pi3k/Akt signaling pathway has the largest difference, so we think Danhong injection may exert its anti-fibrotic effect through Pi3k/Akt signaling pathway. The highest protein content of p-Pi3k and p-Akt was found in the lung tissues of mice in the model group compared with the normal group by Western Blotting; the protein expression of p-Pi3k and p-Akt was significantly reduced after the intervention of Danhong injection compared with the model group ((Fig. 9a, b, c). The Pi3k/Akt signaling pathway, as one of the important signal transduction pathways in cells, plays a key role in inhibiting apoptosis and promoting proliferation by influencing the activation status of various downstream effector molecules, and is closely related to the development of many human diseases[12,13]. Apoptosis is a spontaneous and programmed cell death process that occurs under normal physiological or pathological conditions and is tightly regulated by the body[14]. TUNEL staining is one of the classic methods to detect apoptosis[15]. The staining results showed that the number of apoptotic cells in the lung tissues of mice in the model group was significantly increased. After the intervention of Danhong injection, the number of apoptotic cells was significantly reduced (Fig. 9d). Caspase-3, Caspase-8 and Caspase-9 are the signature proteins of apoptosis[16]. The detection of apoptosis marker proteins in mouse lung tissues revealed that high doses of Danhong injection could reduce the levels of Caspase-3, Caspase-8 and Caspase-9 in lung tissues of mice with PF (Fig. 9e, f, g). These evidences suggest that Danhong

injection may exert its anti-PF effect by inhibiting cell apoptosis through Pi3k/Akt signaling pathway.

Discussion

The onset and progression of PF is mediated by complex factors[17]. In addition to fibroblast-related processes, lung inflammation and oxidative stress play an integral role in promoting the formation of PF[18]. Danhong injection is a compound Chinese herbal injection, the first patented Chinese patent medicine in China to rapidly resolve systemic organ blood supply deficiencies and ischemic infarct disorders, and is commonly used in the treatment of cardiovascular and cerebrovascular diseases[19,20]. Previous studies have confirmed the clinical use of Danhong injection in the treatment of idiopathic PF. It is able to alleviate patients' clinical symptoms and lung function, and no adverse effects have been identified[7].

Based on the clear clinical effectiveness of Danhong injection, we used network pharmacology to explore the material basis and potential mechanisms of action. A topological analysis of the drug's active ingredient and target interaction network revealed that luteolin, baicalin, quercetin, kaempferol and β-sitosterol are the active ingredients that may play an important role in Danhong Injection. Luteolin is a flavonoid with anti-inflammatory and antioxidant properties. It has been reported that luteolin can alleviate PF in both in vitro and in vivo experiments[21]. Quercetin is a biologically active flavonoid and has been shown to inhibit the development of PF by promoting the apoptosis of lung fibroblasts[22]. Baicalein, a flavonoid with anti-

inflammatory and anti-cancer effects, can reduce the conversion of pulmonary fibroblasts to pulmonary myofibroblasts by inhibiting miR-21 levels, thereby inhibiting PF[23]. Kaempferol, a flavonoid widely found in plants and fruits, has anti-inflammatory and anti-fibrotic effects and has been shown to reduce silica-induced PF in mice by modulating autophagy[24]. β-sitosterol can enhance mitochondrial function by promoting internal mitochondrial membrane fluidity, thereby slowing the progression of PF[25,26]. Based on the above results, we concluded that the main active ingredients of Danhong injection had anti-inflammatory, antioxidant and anti-fibrotic effects.

GO and KEGG enrichment showed that Danhong injection may act through the targets of MDM2, IL-2, CCL5, AKT1, MMP9, CASP3 and MMP2. The enrichment pathway results showed that Danhong injection may act through Pi3k/Akt signaling pathway, Jak-STAT signaling pathway, GnRH signaling pathway, ErbB signaling pathway, Rap1 signaling pathway, Ras signaling pathway, NF signaling pathway, FoxO signaling pathway, Apoptosis, MAPK signaling pathway and many other signaling pathways. We found a closer relationship with Pi3k/Akt signaling pathway by extensive qRT-PCR and protein blotting methods. Danhong injection significantly reduced the protein expression of phosphorylated Pi3k and Akt in lung tissue of mice with PF.

The Pi3k protein family is involved in the regulation of various cellular functions such as cell proliferation, differentiation, apoptosis and glucose transport[27]. The Pi3k/Akt signaling pathway was found to activate the receptor tyrosine kinase, which translocated Pi3k from the cytoplasm to the cell membrane, activating and catalyzing

366 the subunit that generates the 2nd messenger PI(3,4,5) P3 that binds to the PH domain
367 at the amino acid terminus of Akt and regulates the expression of the mammalian target
368 of rapamycin downstream[28]. The high expression of NF-κB in early stages of PF is
369 associated with activation of the Pi3k/Akt signaling pathway, and the interaction
370 between the activated MAPK signaling pathway and Pi3k/Akt signaling pathway
371 promotes PF formation. Inhibition of PF by blocking the Pi3k/Akt signaling pathway
372 could potentially be a new direction for the treatment of PF. It was found that Pi3k
373 inhibitors exhibited superior proliferation inhibitory activity against mouse MLG2908
374 lung fibroblasts and were able to improve lung function and pathological damage in
375 mice with PF, and reduce hydroxyproline content and α-SMA levels in lung
376 tissue[29,30]. Our results have demonstrated that Danhong injection can attenuate the
377 protein expression of phosphorylated Pi3k and Akt in the lung tissue of PF mice.
378 Activation of Akt by Pi3k can mediate cell growth induced by insulin, various growth
379 factors, etc. through phosphorylation or inhibition of its downstream target proteins Bad,
380 Caspase9, NF-κB, Forkhead, mTOR, Par-4 and P21, thus promoting cell survival via
381 multiple pathways and exerting anti-apoptotic effects[31–34]. the TUNEL staining
382 results demonstrated that Danhong injection The TUNEL staining results demonstrated
383 that Danhong injection was able to reduce apoptosis in lung tissues. The reduction of
384 Caspase-3, Caspase-8 and Caspase-9 proteins in lung tissues after administration also
385 verified this conclusion. Our results confirm that Danhong injection can inhibit
386 apoptosis through the Pi3k/Akt signaling pathway to exert anti-PF effects. However,
387 fibroblasts and epithelial cells play an important role in pulmonary fibrosis, and lung

tissue contains many types of cells, in which cell apoptosis occurs is currently unknown and this will be the direction of our future research.

Conclusions

In summary, this study was based on a network pharmacology approach to analyze the anti-PF mechanism of Danhong injection with multiple components-multiple targets-multiple pathways-multiple effects, as well as experimental validation. The results suggest that Danhong injection may exert its anti-PF effect by regulating apoptosis through Pi3k/Akt signaling pathway, with a view to providing theoretical and experimental basis for the clinical application of Danhong injection.

Abbreviations

PF: Pulmonary fibrosis; TCMSP: Traditional Chinese Medicine Systems Pharmacology Database and Analysis Platform; TCMID: Traditional Chinese Medicines Integrated Database; SEA: Similarity ensemble approach; UniProt: Universal Protein; DAVID: DAVID Bioinformatics Resources; STRING: STRING databases; OMIM: Online Mendelian Inheritance in Man; CTD: Comparative Toxicogenomics Database; TTD: Therapeutic Target Database; H&E: Haematoxylin and eosin; IHC: Immunohistochemistry; MF: Molecular Function; BP: Biological Process; CC: Cellular Components; qRT-PCR: RNA isolation and quantitative real-time PCR; WB: Western Blotting; ELISA: Enzyme-linked immunosorbent assay; TUNE: Terminal deoxynucleotidyl transferase dUTP nick end labelling; PVDF: Polyvinylidene difuoride; HRP: Horseradish peroxidase; RT: Room temperature ANOVA: A one-way analysis of variance.

411 **Authors' contributions**

412 XZ and JS designed the study; DH and YX wrote the main manuscript text; DW, TH, DH, and YX
413 performed the animal experiments; WP, YX, and DH analysed the data and prepared the figures. All
414 authors read and approved the final manuscript.

415

416 **Funding**

417 This work was supported by National Natural Science Foundation of China (82074358), Jiangsu
418 Provinces colleges and universities (integration of Chinese and Western medicine)

419

420 **Availability of data and materials**

421 The datasets used in the current study are available from the corresponding author on reasonable
422 request.

423

424 **Ethics approval and consent to participate**

425 The animal care and experimental procedures used in the current study were approved by the
426 Institutional Animal Care and Use Committee of the Nanjing University of Chinese Medicine.

427

428 **Consent for publication**

429 Not applicable.

430

431 **Competing interests**

432 The authors declare that they have no competing interests.

Author details

[1]Affiliated Hospital of Nanjing University of Chinese Medicine, Nanjing, 210023 China. [2]Department of Respiratory Medicine, Jiangsu Province Hospital of Chinese Medicine, Nanjing, 210023 China.[3]Jiangsu Key Laboratory of Pediatric Respiratory Disease, Institute of Pediatrics, Affiliated Hospital of Nanjing University of Chinese Medicine, No. 138, Xianlin Avenue, Qixia District, Nanjing, 210023 China.[4]Medical Metabolomics Center, Nanjing University of Chinese Medicine, Nanjing, 210023 China

References

1. Spagnolo P, Kropski JA, Jones MG, Lee JS, Rossi G, Karampitsakos T, et al. Idiopathic pulmonary fibrosis: Disease mechanisms and drug development. Pharmacol Ther. 2021;222:107798.

2. Maher TM, Strek ME. Antifibrotic therapy for idiopathic pulmonary fibrosis: time to treat. Respir Res. 2019;20:205.

3. Sack C, Raghu G. Idiopathic pulmonary fibrosis: unmasking cryptogenic environmental factors. Eur Respir J. England; 2019;53.

4. Zhao Wenqing, Zheng Minyu. Traditional Chinese Medicine and Western Treatment Progress of IPF. Chinese Archives of Traditional Chinese Medicine. 2016;402–5.

5. Zhang Xinyue. Analysis of blood stasis throughout interstitial lung disease. Traditional Chinese Medicinal Research. 2013;1–2.

6. Insufficiency being the source of all diseases and Danhong Injection. Insufficiency being the source of all diseases and Danhong Injection. Clinical Journal of Chinese Medicine. 2015;65–7.

7. Xin Lili, Jiang Miao, Zhang Geng, Gong Jie-ning. Efficacy and safety of Danhong injection for idiopathic pulmonary fibrosis: Meta-analysis. China Journal of Chinese Materia Medica. 2016;3859–65.

8. Xu X, Zhang W, Huang C, Li Y, Yu H, Wang Y, et al. A novel chemometric method for the prediction of human oral bioavailability. Int J Mol Sci. 2012;13:6964–82.

9. Ng B, Dong J, D'Agostino G, Viswanathan S, Widjaja AA, Lim W-W, et al.

Interleukin-11 is a therapeutic target in idiopathic pulmonary fibrosis. Sci Transl Med. United States; 2019;11.

10. Plantier L, Cazes A, Dinh-Xuan A-T, Bancal C, Marchand-Adam S, Crestani B. Physiology of the lung in idiopathic pulmonary fibrosis. Eur Respir Rev. England; 2018;27.

11. Srivastava AK, Khare P, Nagar HK, Raghuwanshi N, Srivastava R. Hydroxyproline: A Potential Biochemical Marker and Its Role in the Pathogenesis of Different Diseases. Curr Protein Pept Sci. United Arab Emirates; 2016;17:596–602.

12. Jafari M, Ghadami E, Dadkhah T, Akhavan-Niaki H. PI3k/AKT signaling pathway: Erythropoiesis and beyond. J Cell Physiol. United States; 2019;234:2373–85.

13. Rahmani M, Nkwocha J, Hawkins E, Pei X, Parker RE, Kmieciak M, et al. Cotargeting BCL-2 and PI3K Induces BAX-Dependent Mitochondrial Apoptosis in AML Cells. Cancer Res. 2018;78:3075–86.

14. Xu X, Lai Y, Hua Z-C. Apoptosis and apoptotic body: disease message and therapeutic target potentials. Biosci Rep. 2019;39.

15. Kyrylkova K, Kyryachenko S, Leid M, Kioussi C. Detection of apoptosis by TUNEL assay. Methods Mol Biol. United States; 2012;887:41–7.

16. Holmes WF, Soprano DR, Soprano KJ. Synthetic retinoids as inducers of apoptosis in ovarian carcinoma cell lines. J Cell Physiol. United States; 2004;199:317–29.

17. Spagnolo P, Kropski JA, Jones MG, Lee JS, Rossi G, Karampitsakos T, et al. Idiopathic pulmonary fibrosis: Disease mechanisms and drug development. Pharmacol Ther. 2021;222:107798.

18. Miao K, Pan T, Mou Y, Zhang L, Xiong W, Xu Y, et al. Scutellarein inhibits BLM-mediated pulmonary fibrosis by affecting fibroblast differentiation, proliferation, and apoptosis. Ther Adv Chronic Dis. 2020;11:2040622320940185.

19. Wan L-M, Tan L, Wang Z-R, Liu S-X, Wang Y-L, Liang S-Y, et al. Preventive and therapeutic effects of Danhong injection on lipopolysaccharide induced acute lung injury in mice. J Ethnopharmacol. Ireland; 2013;149:352–9.

20. Feng X, Li Y, Wang Y, Li L, Little PJ, Xu S-W, et al. Danhong injection in cardiovascular and cerebrovascular diseases: Pharmacological actions, molecular mechanisms, and therapeutic potential. Pharmacol Res. Netherlands; 2019;139:62–75.

21. Chen C-Y, Peng W-H, Wu L-C, Wu C-C, Hsu S-L. Luteolin ameliorates experimental lung fibrosis both in vivo and in vitro: implications for therapy of lung fibrosis. J Agric Food Chem. United States; 2010;58:11653–61.

22. Veith C, Drent M, Bast A, van Schooten FJ, Boots AW. The disturbed redox-balance in pulmonary fibrosis is modulated by the plant flavonoid quercetin. Toxicol Appl Pharmacol. United States; 2017;336:40–8.

23. Cui X, Sun X, Lu F, Jiang X. Baicalein represses TGF-β1-induced fibroblast differentiation through the inhibition of miR-21. Toxicol Appl Pharmacol. United States; 2018;358:35–42.

24. Liu H, Yu H, Cao Z, Gu J, Pei L, Jia M, et al. Kaempferol Modulates Autophagy and Alleviates Silica-Induced Pulmonary Fibrosis. DNA Cell Biol. United States; 2019;38:1418–26.

25. Lee I-A, Kim E-J, Kim D-H. Inhibitory effect of β-sitosterol on TNBS-induced colitis in mice. Planta Med. Germany; 2012;78:896–8.

26. Shi C, Wu F, Xu J. Incorporation of β-sitosterol into mitochondrial membrane enhances mitochondrial function by promoting inner mitochondrial membrane fluidity. J Bioenerg Biomembr. United States; 2013;45:301–5.

27. Su D, Zhou Y, Hu S, Guan L, Shi C, Wang Q, et al. Role of GAB1/PI3K/AKT signaling high glucose-induced cardiomyocyte apoptosis. Biomed Pharmacother. France; 2017;93:1197–204.

28. Mercer PF, Woodcock HV, Eley JD, Platé M, Sulikowski MG, Durrenberger PF, et al. Exploration of a potent PI3 kinase/mTOR inhibitor as a novel anti-fibrotic agent in IPF. Thorax. 2016;71:701–11.

29. Lin S, Jin J, Liu Y, Tian H, Zhang Y, Fu R, et al. Discovery of 4-Methylquinazoline Based PI3K Inhibitors for the Potential Treatment of Idiopathic Pulmonary Fibrosis. J Med Chem. United States; 2019;62:8873–9.

30. Hettiarachchi SU, Li Y-H, Roy J, Zhang F, Puchulu-Campanella E, Lindeman SD, et al. Targeted inhibition of PI3 kinase/mTOR specifically in fibrotic lung fibroblasts suppresses pulmonary fibrosis in experimental models. Sci Transl Med. United States; 2020;12.

31. Jia G, Mitra AK, Gangahar DM, Agrawal DK. Insulin-like growth factor-1 induces phosphorylation of PI3K-Akt/PKB to potentiate proliferation of smooth muscle cells in human saphenous vein. Exp Mol Pathol. 2010;89:20–6.

32. Jung F, Haendeler J, Goebel C, Zeiher AM, Dimmeler S. Growth factor-induced phosphoinositide 3-OH kinase/Akt phosphorylation in smooth muscle cells: induction of cell proliferation and inhibition of cell death. Cardiovasc Res. England; 2000;48:148–57.

33. Xing Y-Q, Li A, Yang Y, Li X-X, Zhang L-N, Guo H-C. The regulation of FOXO1 and its role in disease progression. Life Sci. Netherlands; 2018;193:124–31.

34. Zhang L-N, Zhao L, Yan X-L, Huang Y-H. Loss of G3BP1 suppresses proliferation, migration, and invasion of esophageal cancer cells via Wnt/β-catenin and PI3K/AKT signaling pathways. J Cell Physiol. United States; 2019;234:20469–84.

Figures

Figure 1

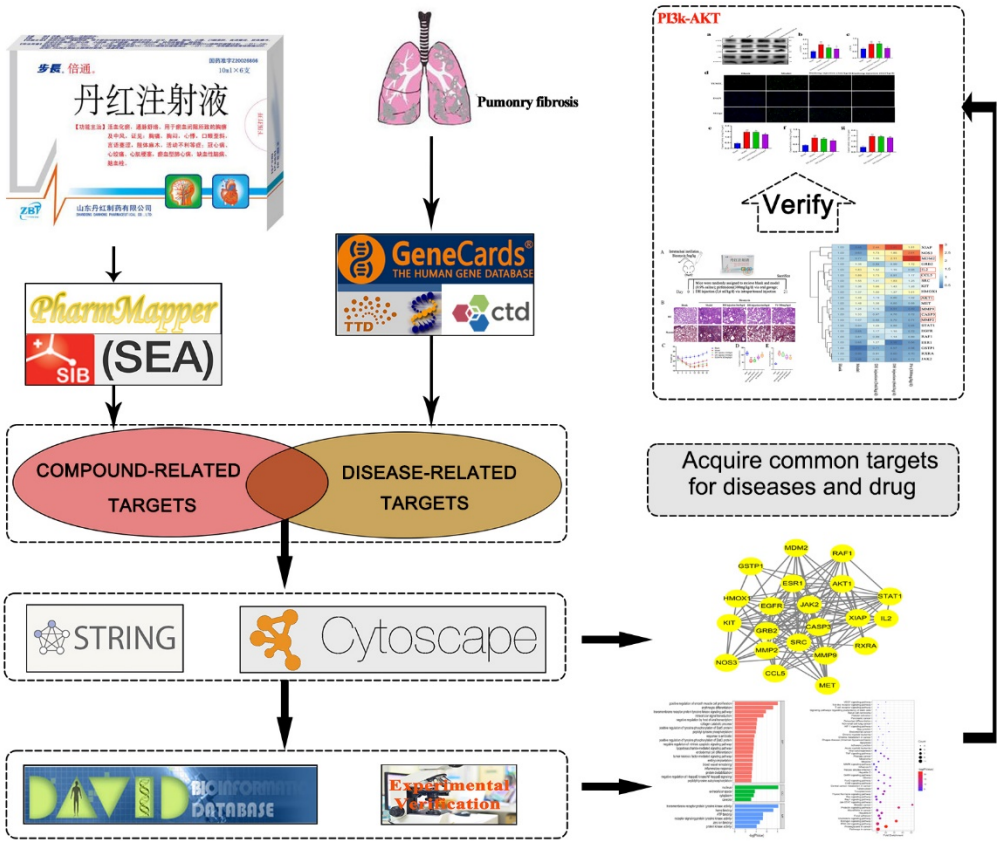

Fig. 1 Technological road-map

Figure 2

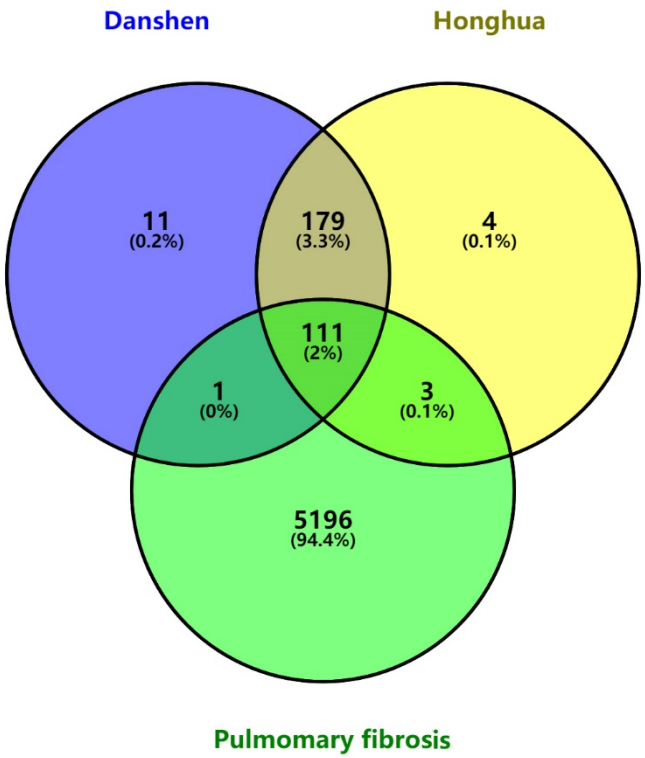

Fig. 2 Drug-disease intersection targets

Figure 3

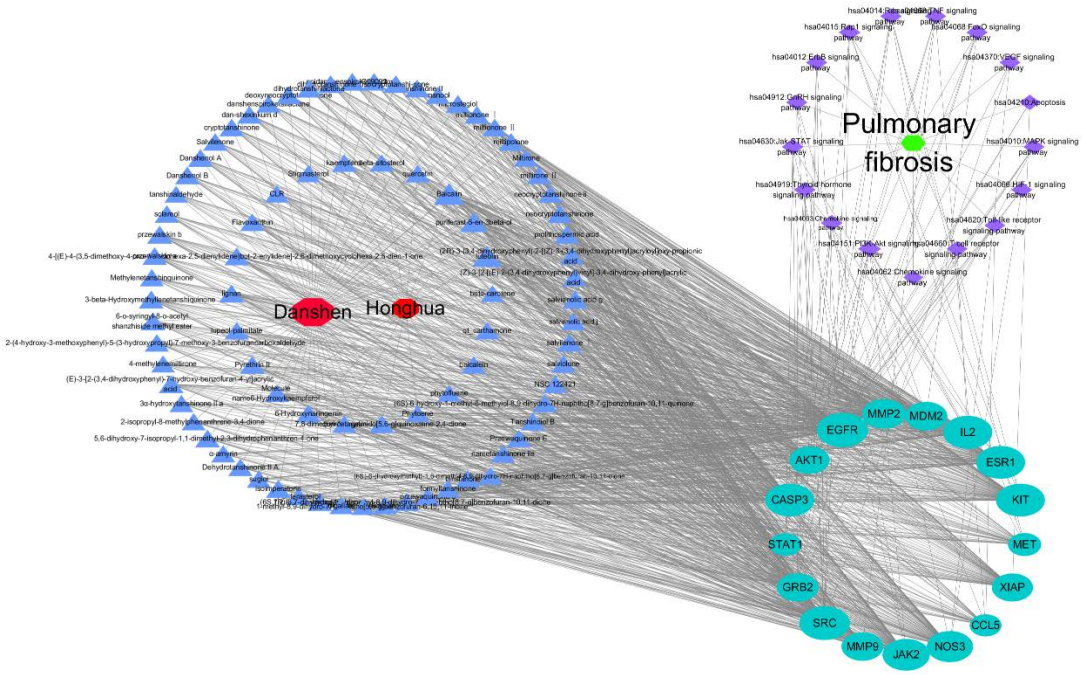

Fig 3 Anti-PF network diagram of the active ingredients of Danhong injection

Figure 4

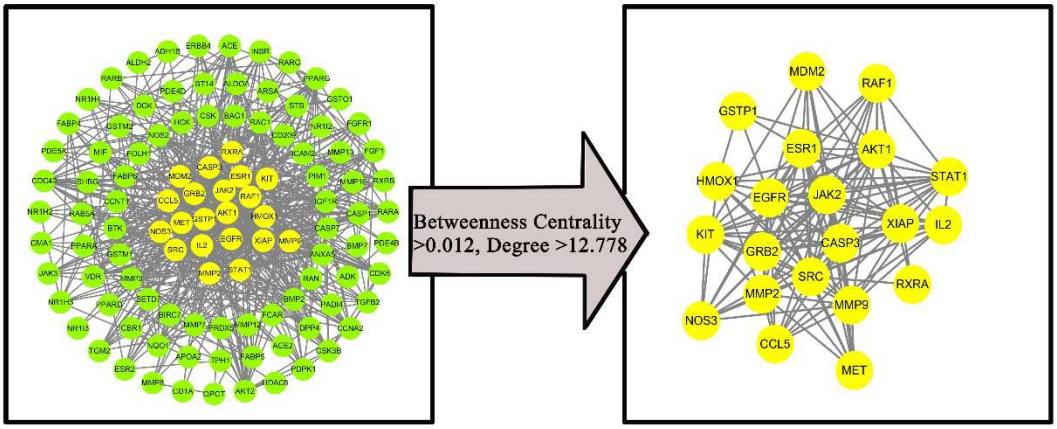

Fig. 4 Screening of the core targets of the active ingredient of Danhong injection against PF

Figure 5

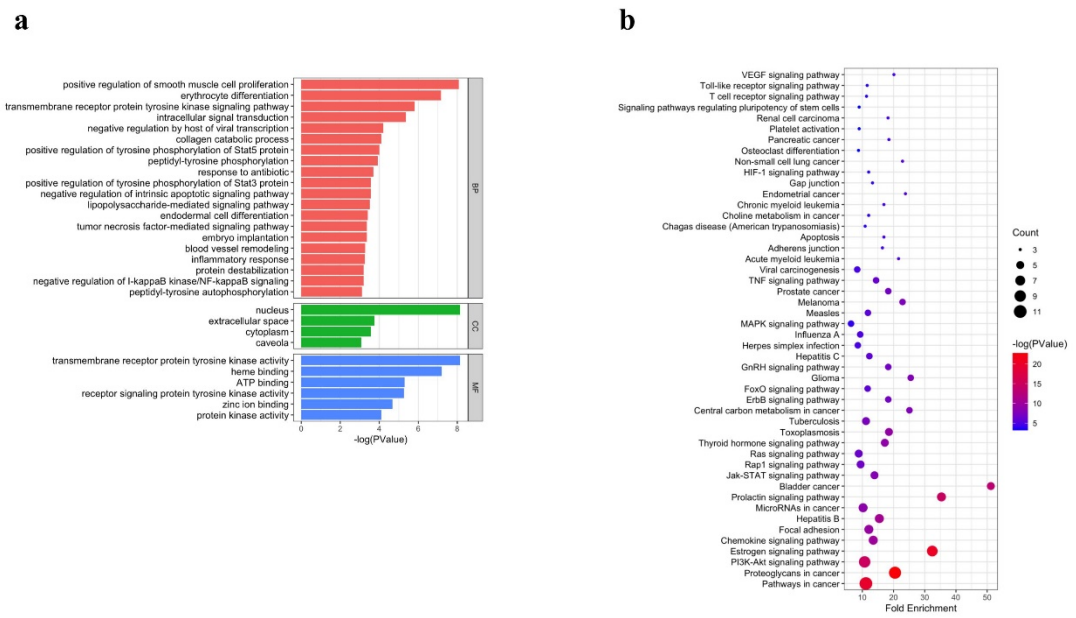

Fig. 5 Anti-PF enrichment analysis of the active ingredients of Danhong injection. a GO enrichment analysis; b KEGG enrichment analysis

Figure 6

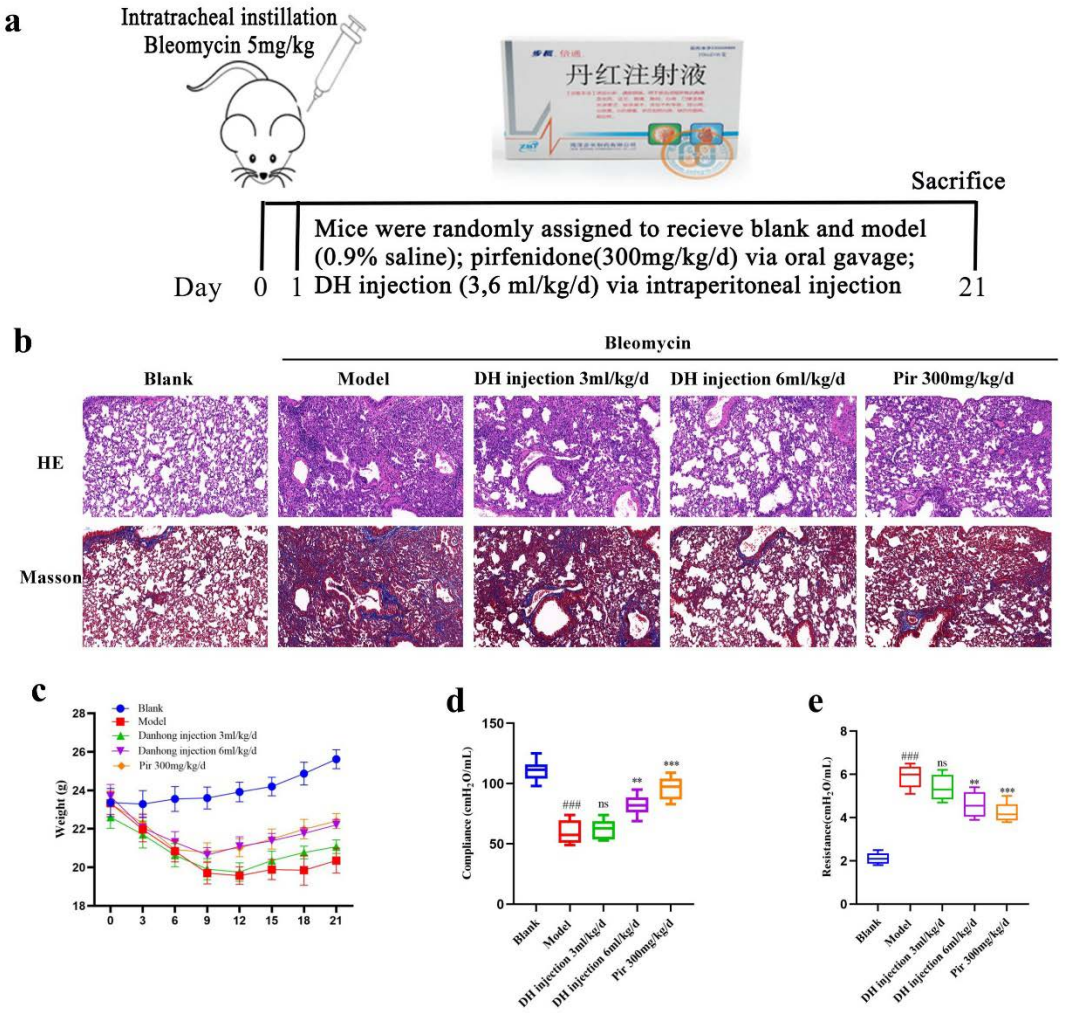

Fig. 6 Danhong injection attenuates bleomycin-induced PF in mice. a Modeling diagram. b. Image of H&E staining and Masson staining obtained at 20×magnifcation in the lung. c Body weight. d Lung compliance. e Lung resistance. All of the data are expressed as mean ± SD (n=6), $^{###}$P<0.01 compared with blank group *P<0.05 compared with model group, **P<0.01 compared with model group, ***P<0.001 compared with model group and ns = no significant compared with model group. Scale bar=50 μm

Figure 7

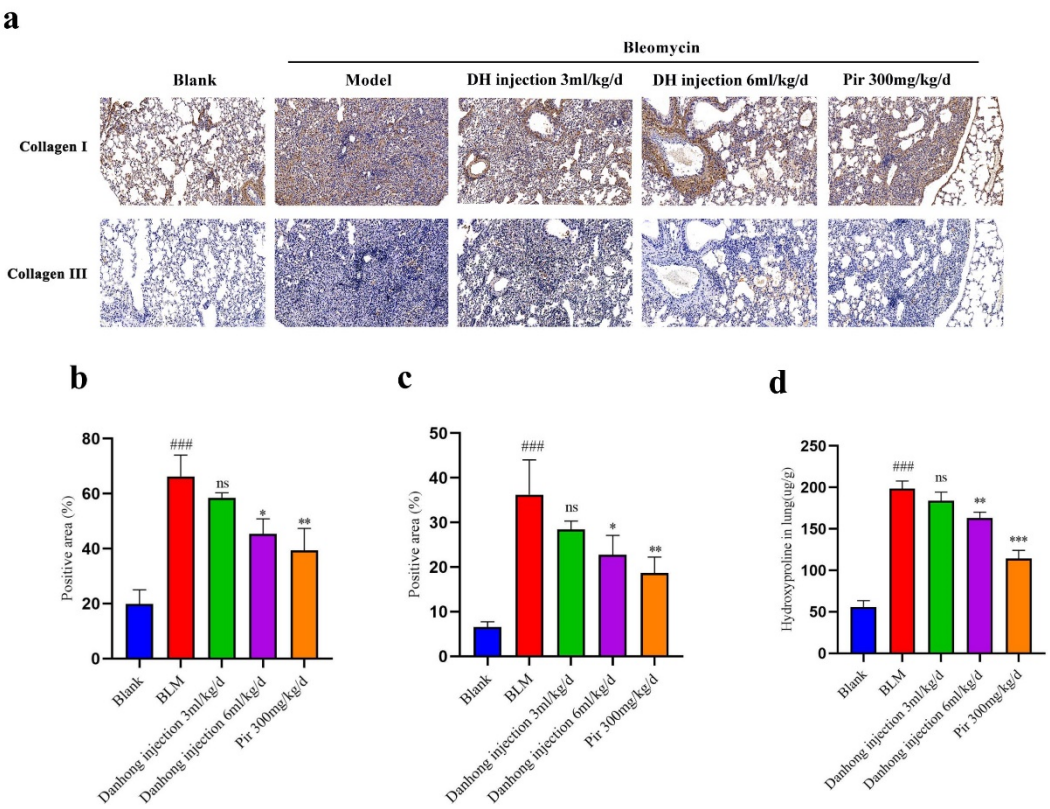

Fig.7 Dan Hong Injection reduced collagen deposition in the lungs of mice with bleomycin-induced PF. a. immunohistochemistry staining of Collagen I and collagen III in lung and image of immunohistochemistry obtained at 20×magnifcation in lung. b, c Histology score of the pulmonary fibrosis calculated by Collagen I and collagen III. d Contents of Hydroxyproline in lung tissue. All of the data are expressed as mean ± SD (n=6), $^{###}$P<0.001 compared with blank group *P<0.5 compared with model group, **P<0.01 compared with model group, ***P<0.001 compared with model group and ns = no significant compared with model group. Scale bar=50 μm

Figure 8

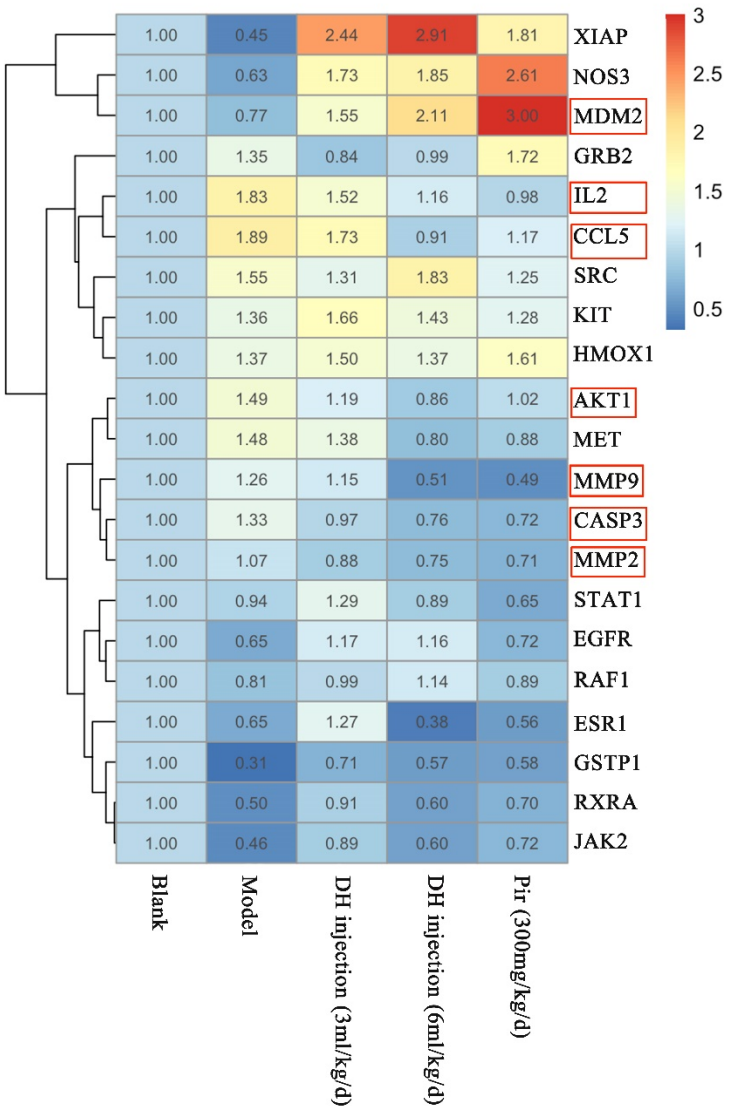

Fig.8 Effect of Danhong injection on the transcription of key target genes in lung tissue of mice with PF. Real-time qPCR analysis of genes, relative expression of XIAP, NOS3, MDM2, GRB2, IL-2, CCL5, SRC, KIT, HMOX1, AKT1, MET, MMP9, CASP3, MMP2, STAT1, EGFR, RAF1, ESR1, GSTP1, RXRA, JAK2 and make a heatmap. All of the data are expressed as mean ± SD (n=3).

Figure 9

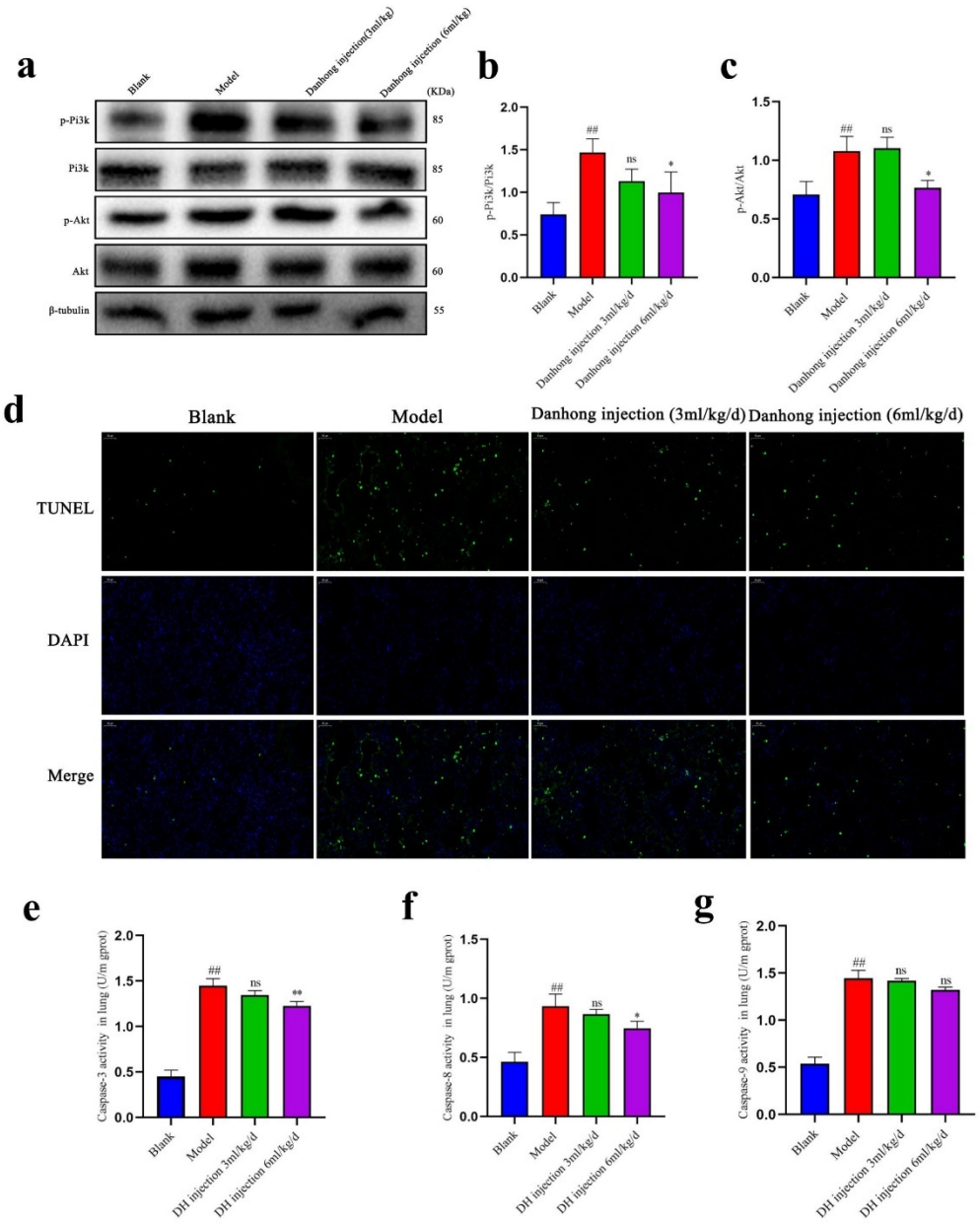

Fig.9 Danhong injection exerts antifibrotic effects via Pi3k/Akt signaling pathway. a b, c Western blotting of p-Pi3k, Pi3k, p-Akt, Akt, and β-tubulin protein in lung. d Immunofluorescence staining of apoptotic cell. DAPI was used to stain the nucleus. d, e, f Contents of Caspase -3、Caspase-8、Caspase-9 in lung tissue. All of the data are expressed as mean ± SD (n=3), $^{\#\#}P<0.01$ compared with blank group $^{*}P<0.05$ compared with model group $^{**}P<0.01$ compared with model group and ns = no significant compared with model group. Scale bar=50 μm

730 **Tables**

731

732 **Table 1** Primer sequences. This is where the description of the table should go

Gene	Forward Primer	Reveres Primer
GAPDH	GGTTGTCTCCTGCGACTTCA	TGGTCCAGGGTTTCTTACTCC
XIAP	ATATGAAGCACGGATCGTTACT	CTTTATCGCCTTCACCTAAAGC
NOS3	CTGAGAGCCTGCAATTACTACC	TTTCCACAGAGAGGATTGTAGC
MDM2	TCTGATCAGTTTAGCGTGGAAT	ATCGCTTTCTCCTGTCTGATAG
GRB2	ATAAGGCAGAACTCAATGGGAA	ACATCATTTCCAAACTTGACGG
IL-2	TGAGCAGGATGGAGAATTACAG	CAGAGGTCCAAGTTCATCTTCT
CCL5	GTATTTCTACACCAGCAGCAAG	TCTTGAACCCACTTCTTCTCTG
SRC	CTATGTGGAGCGGATGAACTAT	ATTCGTTGTCTTCTATGAGCCG
KIT	CAAGAGTTCCGCCTTCTTTAAC	GTGATCATAAGGAAGTTGCGTC
HMOX1	TCCTTGTACCATATCTACACGG	GAGACGCTTTACATAGTGCTGT
AKT1	TGCACAAACGAGGGGAATATAT	CGTTCCTTGTAGCCAATAAAGG
MET	TCACTATCTACCTGTTGCAAGG	CAGCATTTTAGCATCACTTCGT
MMP9	CAAAGACCTGAAAACCTCCAAC	GACTGCTTCTCTCCCATCATC
CASP3	GAAACTCTTCATCATTCAGGCC	GCGAGTGAGAATGTGCATAAAT
MMP2	ACTTTGAGAAGGATGGCAAGTA	CTTCTTATCCCGGTCATAGTCC
STAT1	GATCCGTCAGCAGCTTAAAAAG	CTGACAACACCTGCTTGTTTTT
EGFR	TGAGTTCTCTGAGTGCAACTAG	GAATGCGTCATCTATGTTGTCC
RAF1	ACATCAACAACCGAGACCAGATCATC	CACAGTCAGCCACCAACCTCTTC
ESR1	CTACTACCTGGAGAACGAGC	GCGTCGATTGTCAGAATTAGAC
GSTP1	AGCTGGAAGGAGGAGGTGGTTAC	AGGTGTCTCAAGATGGCATTAGATTGG
RXRA	GAGCAGCACTGAGGATATCAAG	GAAGGAGGCCATATTTCCTGAG
JAK2	GAGCAGCACTGAGGATATCAAG	GAAGGAGGCCATATTTCCTGAG

733

734 **Table 2** Active ingredients of compounds. This is where the description of the table
735 should go

Molecular ID	Chemical name	OB%	DL	Herbal
MOL001601	1,2,5,6-tetrahydrotanshinone	38.75	0.36	Radix Salviae
MOL001659	Poriferasterol	43.83	0.76	Radix Salviae
MOL001771	poriferast-5-en-3beta-ol	36.91	0.75	Radix Salviae
MOL001942	isoimperatorin	45.46	0.23	Radix Salviae
MOL002222	sugiol	36.11	0.28	Radix Salviae
MOL002651	Dehydrotanshinone II A	43.76	0.4	Radix Salviae
MOL002776	Baicalin	40.12	0.75	Radix Salviae
				Carthami Flos
MOL000569	digallate	61.85	0.26	Radix Salviae
MOL000006	luteolin	36.16	0.25	Radix Salviae
				Carthami Flos
MOL006824	α-amyrin	39.51	0.76	Radix Salviae
MOL007036	5,6-dihydroxy-7-isopropyl-1,1-dimethyl-2,3-dihydrophenanthren-4-one	33.77	0.29	Radix Salviae
MOL007041	2-isopropyl-8-methylphenanthrene-3,4-dione	40.86	0.23	Radix Salviae

MOL007045	3α-hydroxytanshinone Ⅱa	44.93	0.44	Radix Salviae
MOL007048	(E)-3-[2-(3,4-dihydroxyphenyl)-7-hydroxy-benzofuran-4-yl]acrylic acid	48.24	0.31	Radix Salviae
MOL007049	4-methylenemiltirone	34.35	0.23	Radix Salviae
MOL007050	2-(4-hydroxy-3-methoxyphenyl)-5-(3-hydroxypropyl)-7-methoxy-3-benzofurancarboxaldehyde	62.78	0.4	Radix Salviae
MOL007051	6-o-syringyl-8-o-acetyl shanzhiside methyl ester	46.69	0.71	Radix Salviae
MOL007058	formyltanshinone	73.44	0.42	Radix Salviae
MOL007059	3-beta-Hydroxymethyllenetanshiquinone	32.16	0.41	Radix Salviae
MOL007061	Methylenetanshinquinone	37.07	0.36	Radix Salviae
MOL007063	przewalskin a	37.11	0.65	Radix Salviae
MOL007064	przewalskin b	110.32	0.44	Radix Salviae
MOL007068	Przewaquinone B	62.24	0.41	Radix Salviae
MOL007069	przewaquinone c	55.74	0.4	Radix Salviae
MOL007070	(6S,7R)-6,7-dihydroxy-1,6-dimethyl-8,9-dihydro-7H-naphtho[8,7-g]benzofuran-10,11-dione	41.31	0.45	Radix Salviae
MOL007071	przewaquinone f	40.31	0.46	Radix Salviae
MOL007077	sclareol	43.67	0.21	Radix Salviae
MOL007079	tanshinaldehyde	52.47	0.45	Radix Salviae
MOL007081	Danshenol B	57.95	0.56	Radix Salviae
MOL007082	Danshenol A	56.97	0.52	Radix Salviae
MOL007085	Salvilenone	30.38	0.38	Radix Salviae
MOL007088	cryptotanshinone	52.34	0.4	Radix Salviae
MOL007093	dan-shexinkum d	38.88	0.55	Radix Salviae
MOL007094	danshenspiroketallactone	50.43	0.31	Radix Salviae
MOL007098	deoxyneocryptotanshinone	49.4	0.29	Radix Salviae
MOL007100	dihydrotanshinlactone	38.68	0.32	Radix Salviae
MOL007101	dihydrotanshinone Ⅰ278.32	45.04	0.36	Radix Salviae
MOL007105	epidanshenspiroketallactone	68.27	0.31	Radix Salviae
MOL007107	C09092	36.07	0.25	Radix Salviae
MOL007108	isocryptotanshi-none	54.98	0.39	Radix Salviae
MOL007111	Isotanshinone II	49.92	0.4	Radix Salviae
MOL007115	manool	45.04	0.2	Radix Salviae
MOL007118	microstegiol	39.61	0.28	Radix Salviae
MOL007119	miltionone Ⅰ	49.68	0.32	Radix Salviae
MOL007120	miltionone Ⅱ	71.03	0.44	Radix Salviae
MOL007121	miltipolone	36.56	0.37	Radix Salviae
MOL007122	Miltirone	38.76	0.25	Radix Salviae
MOL007123	miltirone Ⅱ	44.95	0.24	Radix Salviae
MOL007124	neocryptotanshinone ii	39.46	0.23	Radix Salviae
MOL007125	neocryptotanshinone	52.49	0.32	Radix Salviae
MOL007127	1-methyl-8,9-dihydro-7H-naphtho[5,6-g]benzofuran-6,10,11-trione	34.72	0.37	Radix Salviae
MOL007130	prolithospermic acid	64.37	0.31	Radix Salviae
MOL007132	(2R)-3-(3,4-dihydroxyphenyl)-2-[(Z)-3-(3,4-dihydroxyphenyl)acryloyl]oxy-propionic acid	109.38	0.35	Radix Salviae

MOL007140	(Z)-3-[2-[(E)-2-(3,4-dihydroxyphenyl)vinyl]-3,4-dihydroxy-phenyl]acrylic acid	88.54	0.26	Radix Salviae
MOL007141	salvianolic acid g	45.56	0.61	Radix Salviae
MOL007142	salvianolic acid j	43.38	0.72	Radix Salviae
MOL007143	salvilenone Ⅰ	32.43	0.23	Radix Salviae
MOL007145	salviolone	31.72	0.24	Radix Salviae
MOL007149	NSC 122421	34.49	0.28	Radix Salviae
MOL007150	(6S)-6-hydroxy-1-methyl-6-methylol-8,9-dihydro-7H-naphtho[8,7-g]benzofuran-10,11-quinone	75.39	0.46	Radix Salviae
MOL007151	Tanshindiol B	42.67	0.45	Radix Salviae
MOL007152	Przewaquinone E	42.85	0.45	Radix Salviae
MOL007154	tanshinone iia	49.89	0.4	Radix Salviae
MOL007155	(6S)-6-(hydroxymethyl)-1,6-dimethyl-8,9-dihydro-7H-naphtho[8,7-g]benzofuran-10,11-dione	65.26	0.45	Radix Salviae
MOL007156	tanshinone Ⅵ	45.64	0.3	Radix Salviae
MOL001771	poriferast-5-en-3beta-ol	36.91	0.75	Carthami Flos
MOL002680	Flavoxanthin	60.41	0.56	Carthami Flos
MOL002694	4-[(E)-4-(3,5-dimethoxy-4-oxo-1-cyclohexa-2,5-dienylidene)but-2-enylidene]-2,6-dimethoxycyclohexa-2,5-dien-1-one	48.47	0.36	Carthami Flos
MOL002695	lignan	43.32	0.65	Carthami Flos
MOL002698	lupeol-palmitate	33.98	0.32	Carthami Flos
MOL002706	Phytoene	39.56	0.5	Carthami Flos
MOL002707	phytofluene	43.18	0.5	Carthami Flos
MOL002710	Pyrethrin II	48.36	0.35	Carthami Flos
MOL002712	6-Hydroxykaempferol	62.13	0.27	Carthami Flos
MOL002714	baicalein	33.52	0.21	Carthami Flos
MOL002717	qt_carthamone	51.03	0.2	Carthami Flos
MOL002719	6-Hydroxynaringenin	33.23	0.24	Carthami Flos
MOL002721	quercetagetin	45.01	0.31	Carthami Flos
MOL002757	7,8-dimethyl-1H-pyrimido[5,6-g]quinoxaline-2,4-dione	45.75	0.19	Carthami Flos
MOL002773	beta-carotene	37.18	0.58	Carthami Flos
MOL000358	beta-sitosterol	36.91	0.75	Carthami Flos
MOL000422	kaempferol	41.88	0.24	Carthami Flos
MOL000449	Stigmasterol	43.83	0.76	Carthami Flos
MOL000953	CLR	37.87	0.68	Carthami Flos
MOL000098	quercetin	46.43	0.28	Carthami Flos

736
737

Figures

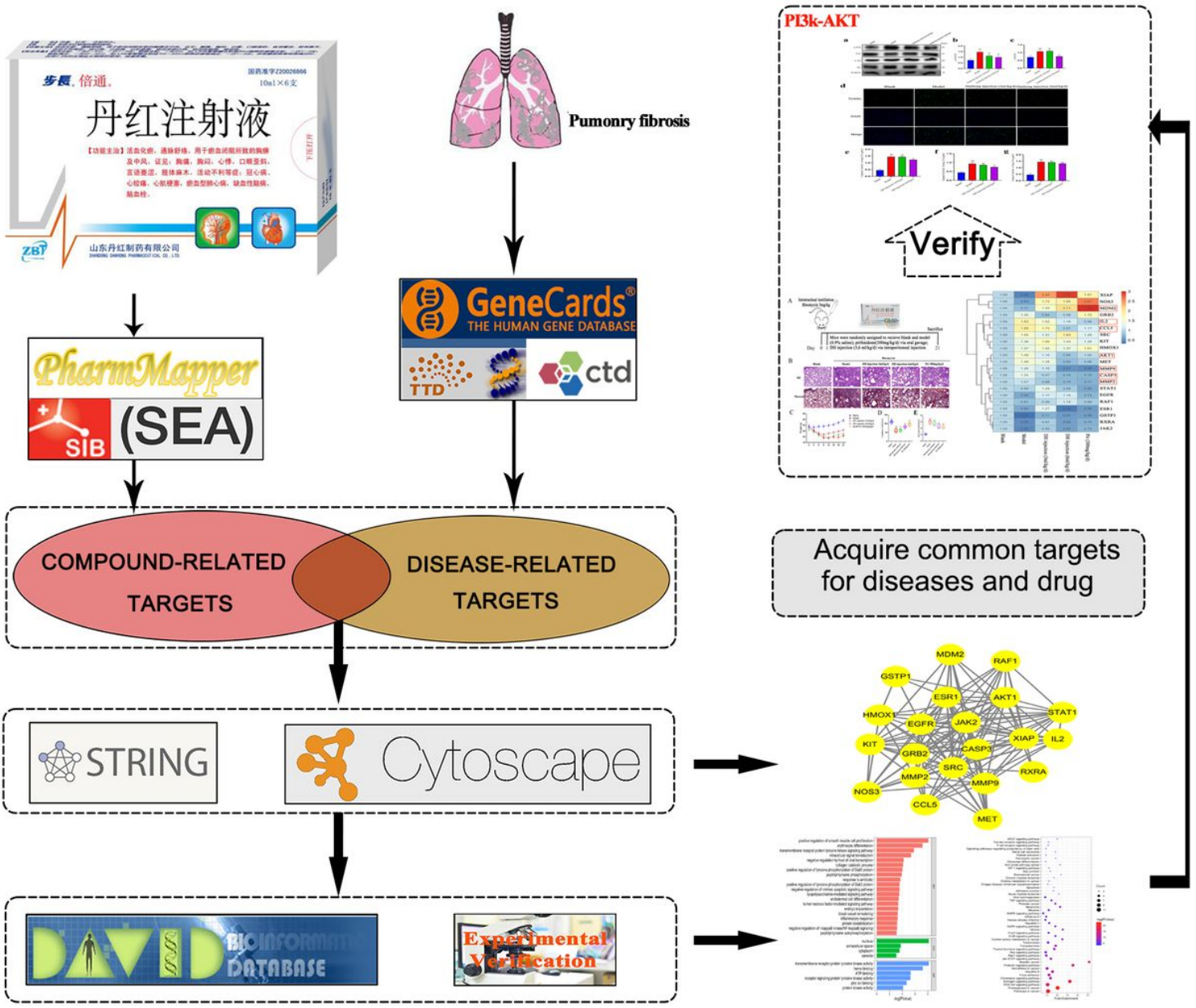

Figure 1

Technological road-map

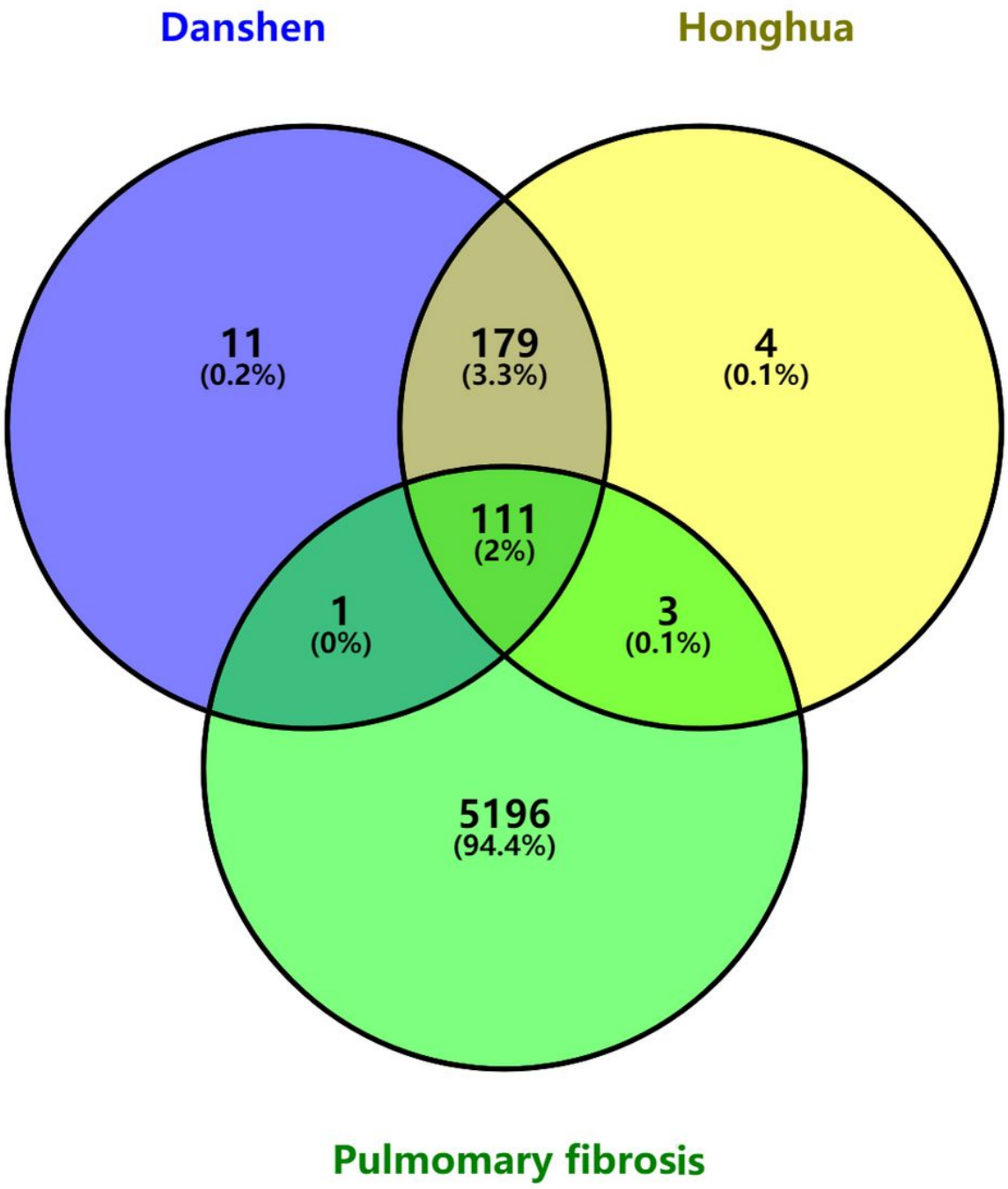

Figure 2

Drug-disease intersection targets

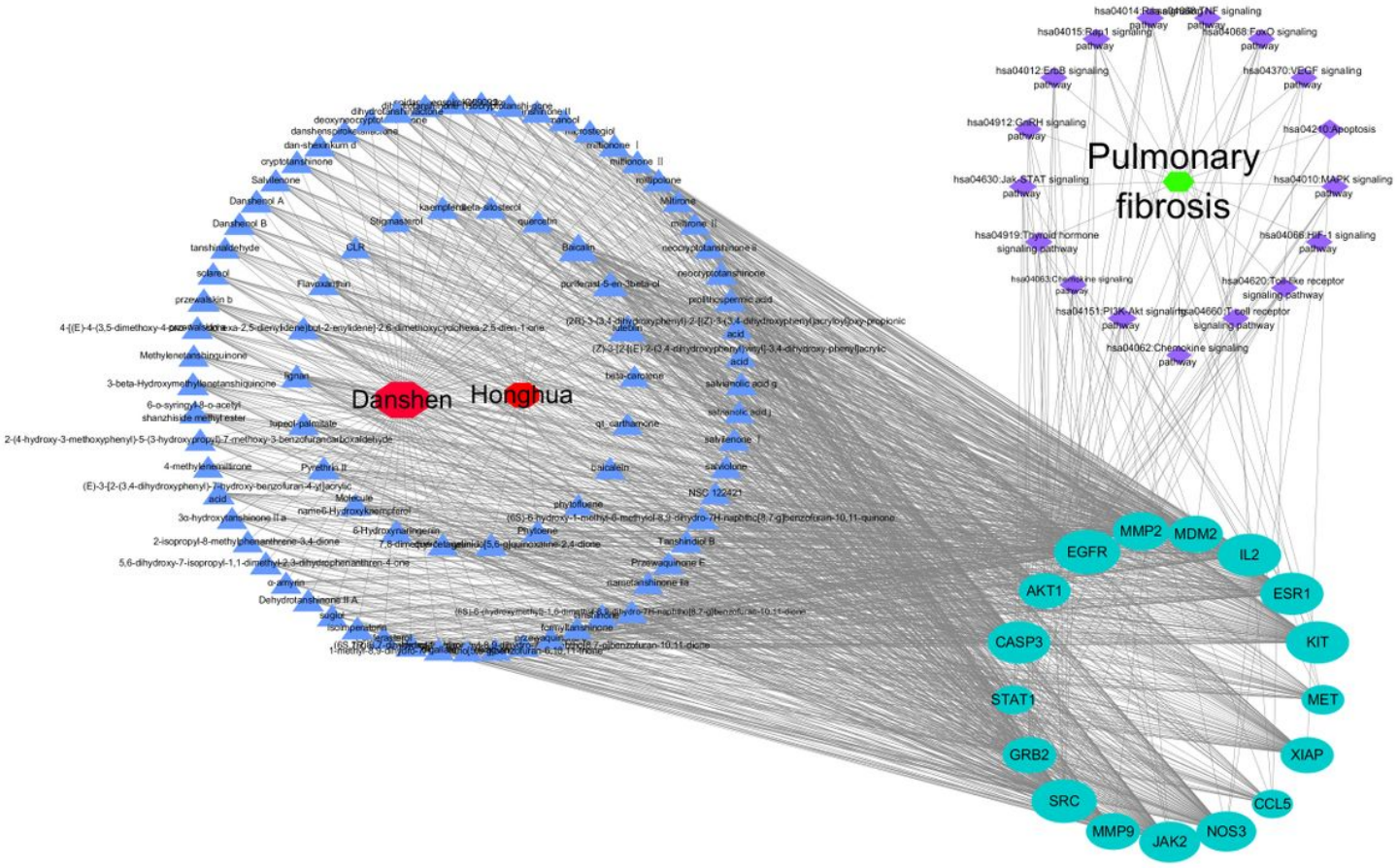

Figure 3

Anti-PF network diagram of the active ingredients of Danhong injection

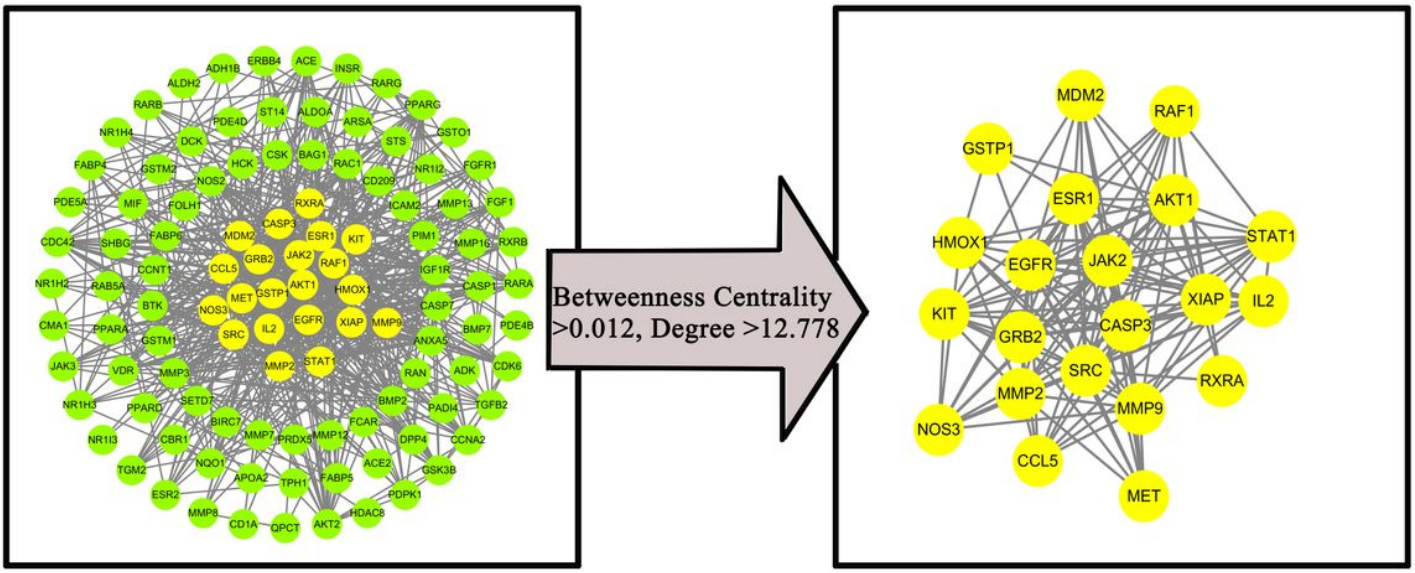

Figure 4

Screening of the core targets of the active ingredient of Danhong injection against PF

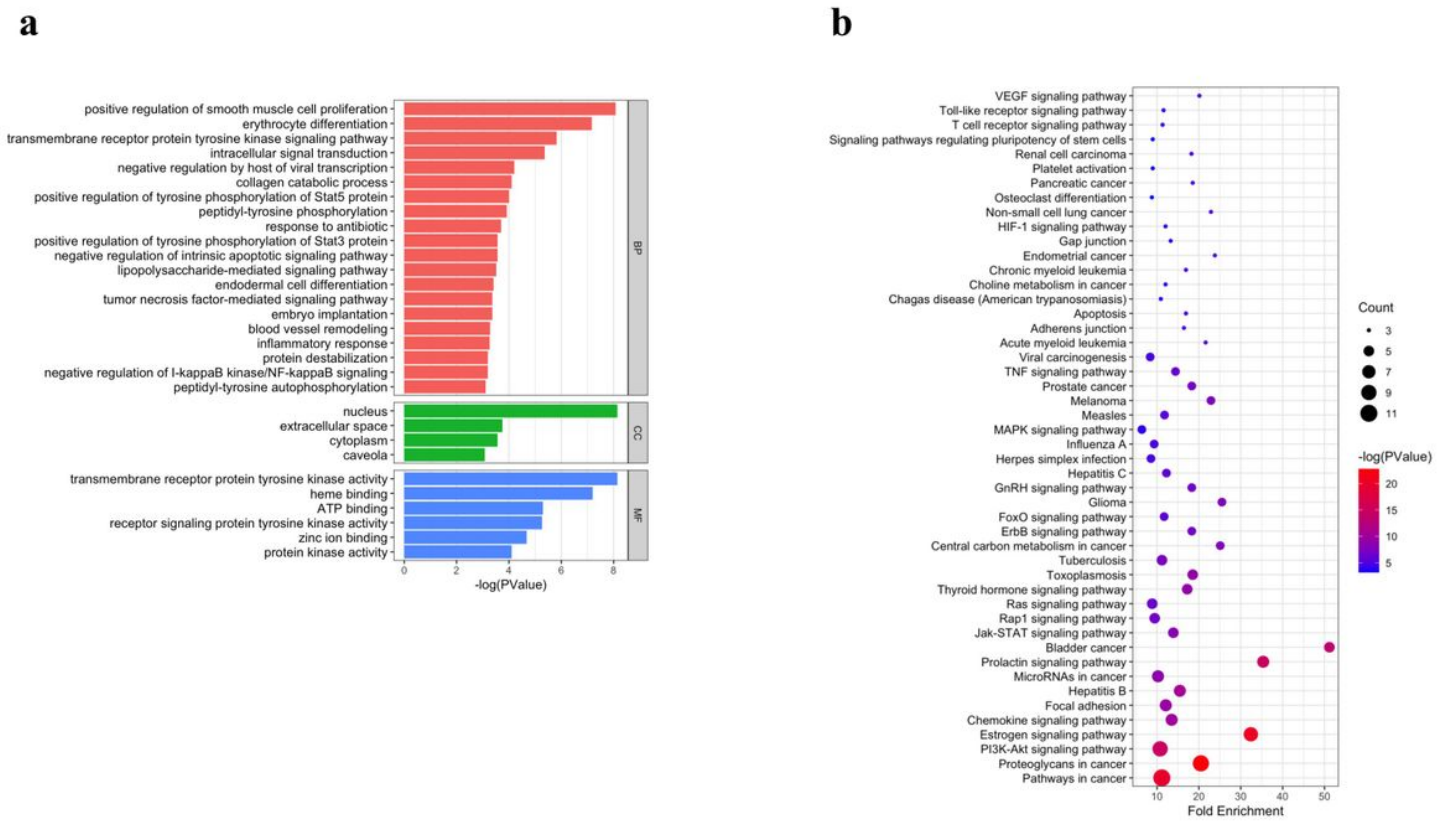

Figure 5

Anti-PF enrichment analysis of the active ingredients of Danhong injection. a GO enrichment analysis; b KEGG enrichment analysis

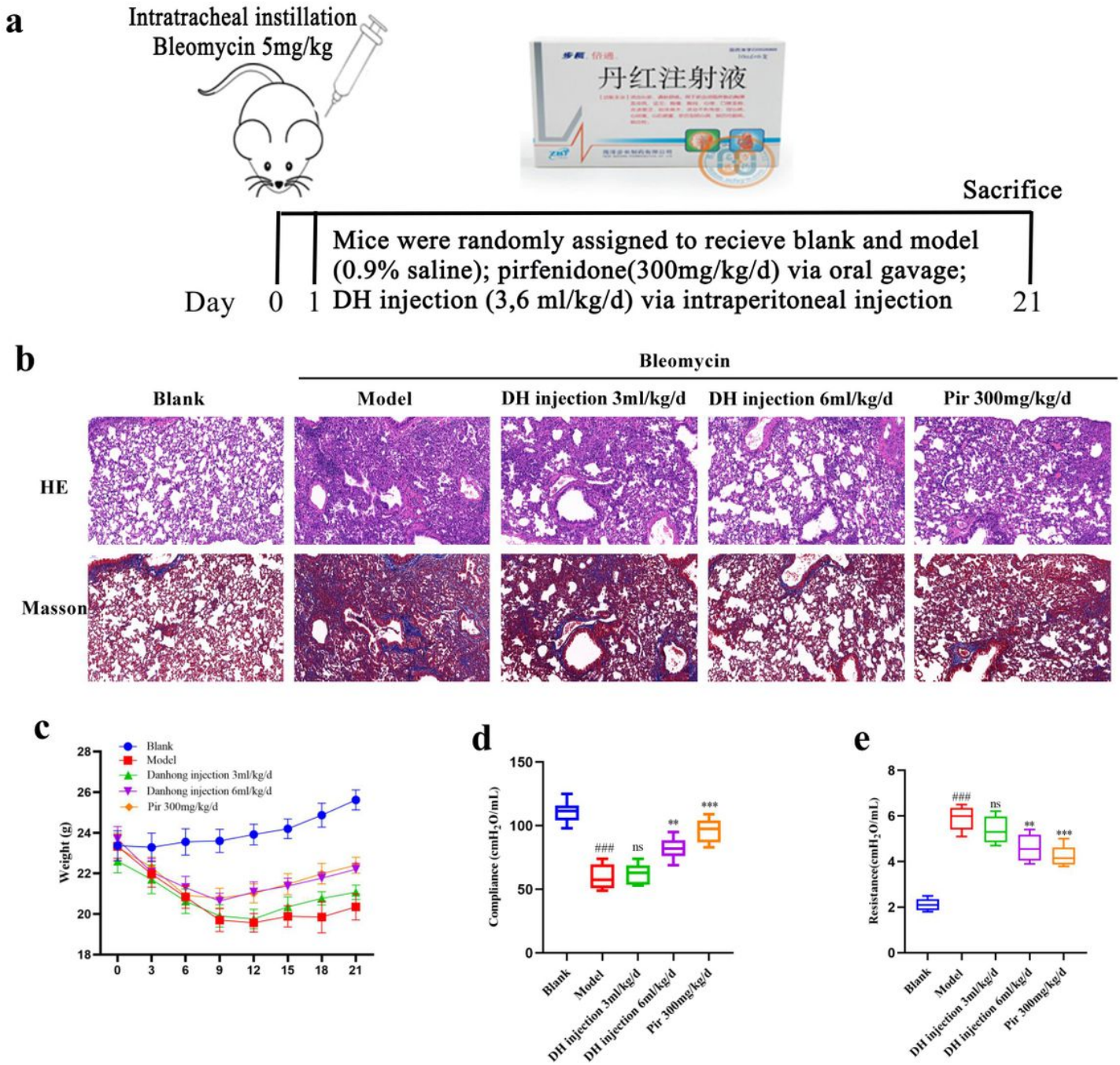

Figure 6

Danhong injection attenuates bleomycin-induced PF in mice. a Modeling diagram. b. Image of H&E staining and Masson staining obtained at 20×magnifcation in the lung. c Body weight. d Lung compliance. e Lung resistance. All of the data are expressed as mean ± SD (n=6), ###P<0.01 compared with blank group *P<0.05 compared with model group, **P<0.01 compared with model group, ***P<0.001 compared with model group and ns = no significant compared with model group. Scale bar=50 μm

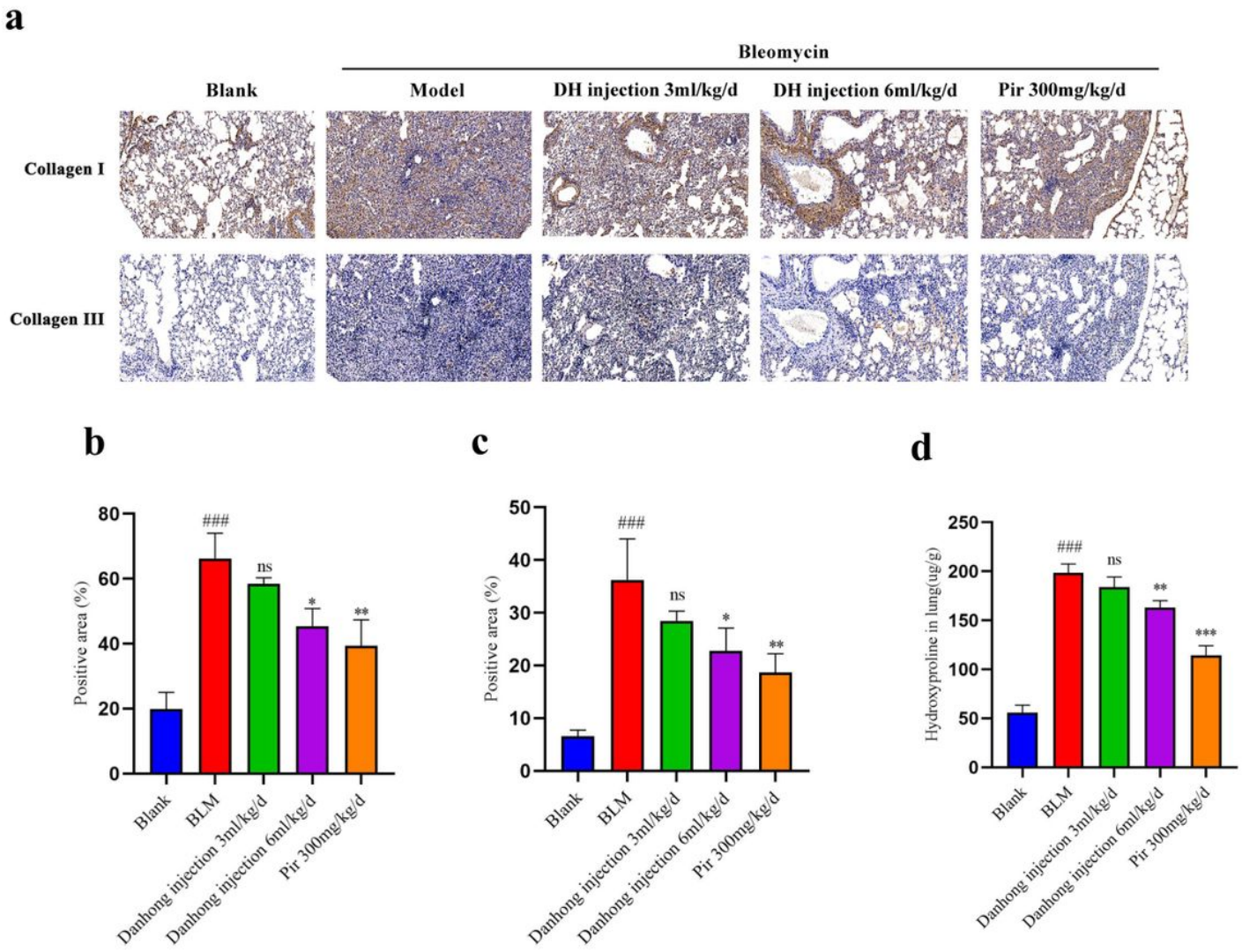

Figure 7

Dan Hong Injection reduced collagen deposition in the lungs of mice with bleomycin-induced PF. a. immunohistochemistry staining of Collagen I and collagen III in lung and image of immunohistochemistry obtained at 20×magnifcation in lung. b, c Histology score of the pulmonary fibrosis calculated by Collagen I and collagen III. d Contents of Hydroxyproline in lung tissue. All of the data are expressed as mean ± SD (n=6), ###P<0.001 compared with blank group *P<0.5 compared with model group, **P<0.01 compared with model group, ***P<0.001 compared with model group and ns = no significant compared with model group. Scale bar=50 μm

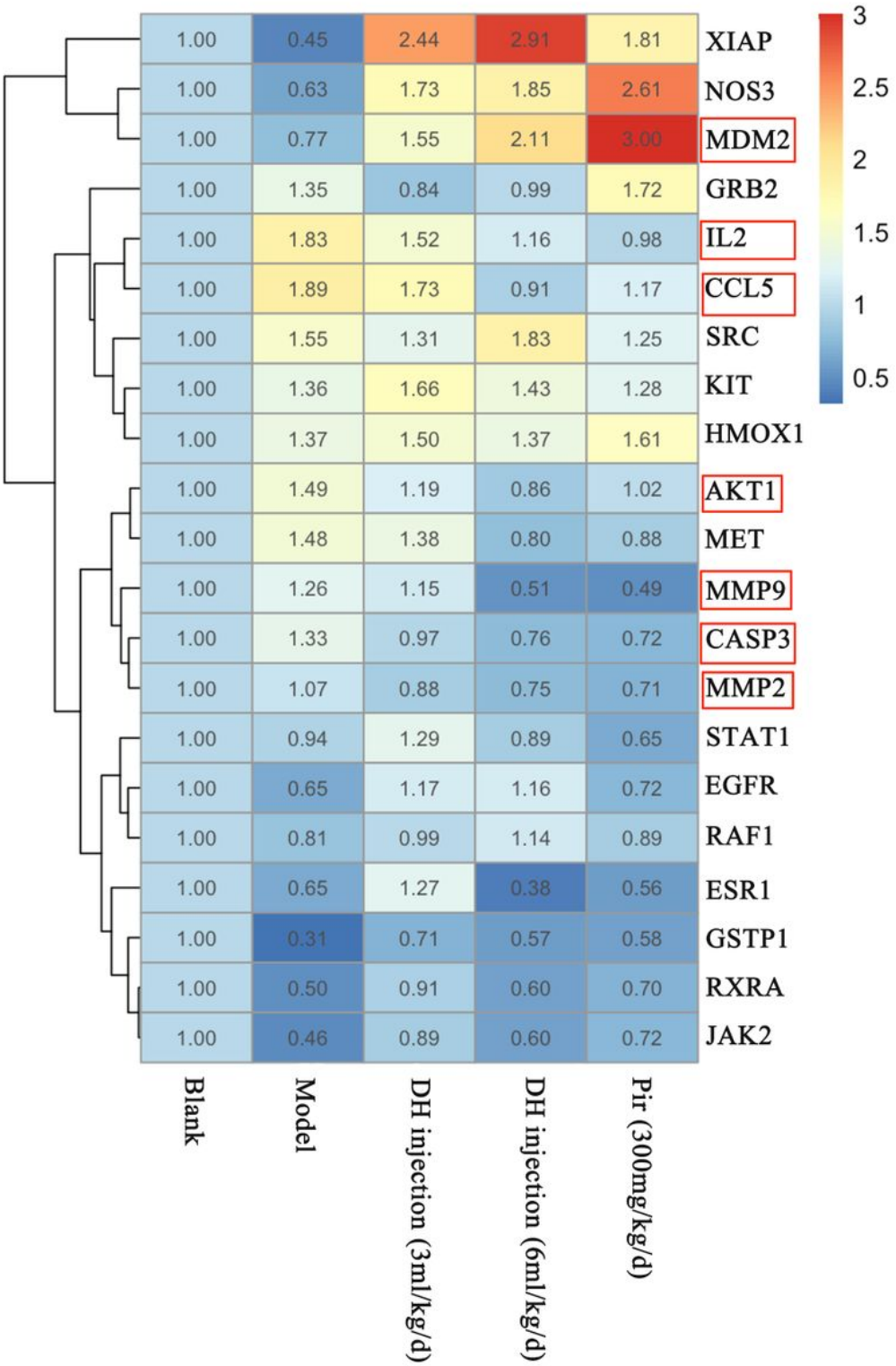

Figure 8

Effect of Danhong injection on the transcription of key target genes in lung tissue of mice with PF. Real-time qPCR analysis of genes, relative expression of XIAP, NOS3, MDM2, GRB2, IL-2, CCL5, SRC, KIT, HMOX1, AKT1, MET, MMP9, CASP3, MMP2, STAT1, EGFR, RAF1, ESR1, GSTP1, RXRA, JAK2 and make a heatmap. All of the data are expressed as mean ± SD (n=3).

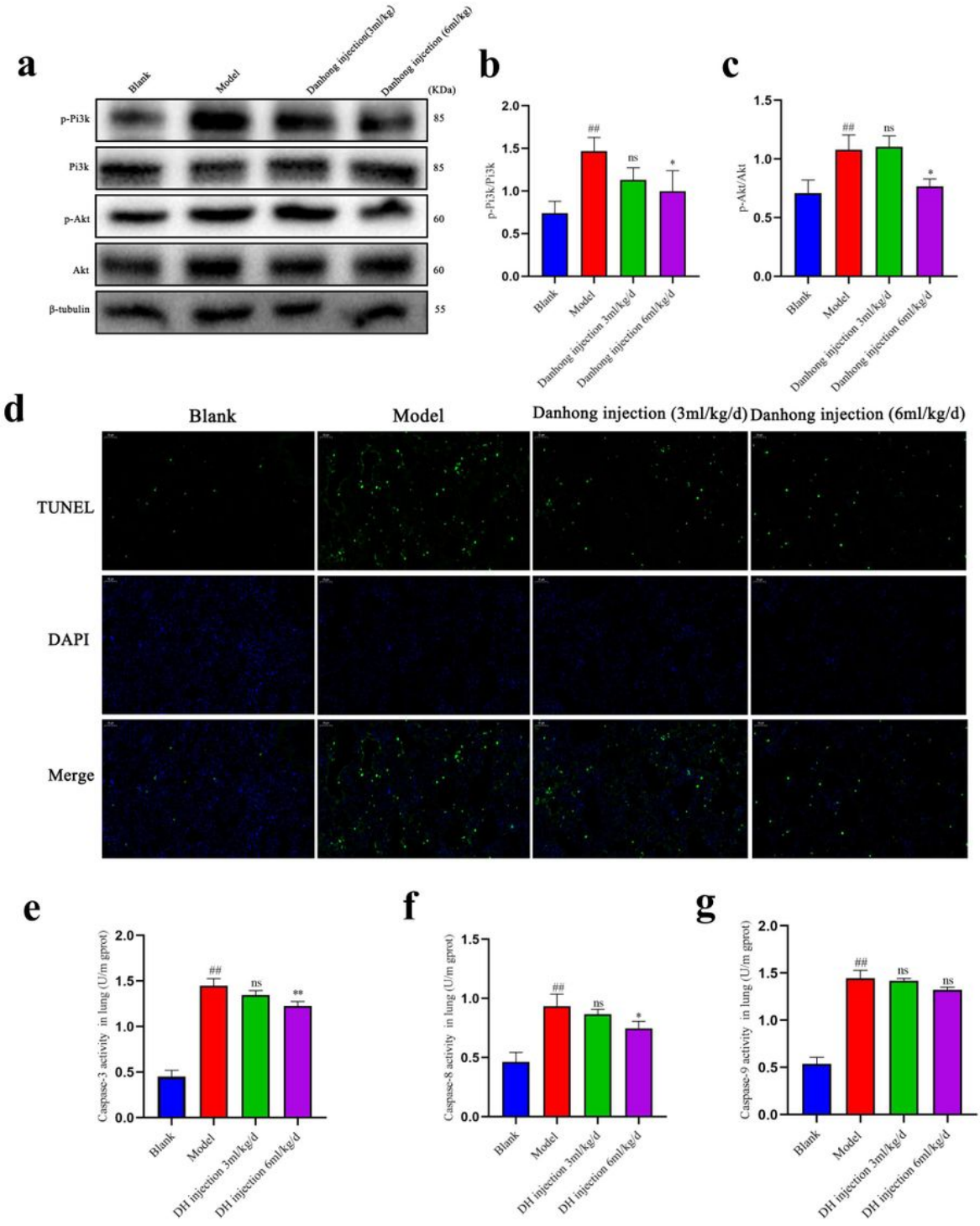

Figure 9

Danhong injection exerts antifibrotic effects via Pi3k/Akt signaling pathway. a b, c Western blotting of p-Pi3k, Pi3k, p-Akt, Akt, and β-tubulin protein in lung. d Immunofluorescence staining of apoptotic cell. DAPI was used to stain the nucleus. d, e, f Contents of Caspase -3. Caspase-8Caspase-9 in lung tissue. All of the data are expressed as mean ± SD (n=3), ##P<0.01 compared with blank group *P<0.05 compared

with model group **P<0.01 compared with model group and ns = no significant compared with model group. Scale bar=50 μm